

Iterative Registration of 3D LADAR Data for Autonomous Navigation¹

R. Madhavan

Intelligent Systems Division
Manufacturing Engineering Laboratory
National Institute of Standards and Technology
Gaithersburg, MD 20899-8230, U.S.A.
raj.madhavan@nist.gov

E. Messina

Intelligent Systems Division
Manufacturing Engineering Laboratory
National Institute of Standards and Technology
Gaithersburg, MD 20899-8230, U.S.A.
elena.messina@nist.gov

Abstract

This paper describes an iterative algorithm for registration of 3D LADAR data. The proposed approach is iconic in nature with suitable modifications to deal with false/spurious matches, occlusions and outliers. Experimental results using data obtained from field trials on an eXperimental Unmanned Vehicle (XUV) are presented to demonstrate the efficacy of the approach. The paper also details ongoing research efforts to determine the feasibility of employing the algorithm for real-time autonomous navigation.

1 Introduction

The Demo III [10] eXperimental Unmanned Vehicle (XUV) (shown in Figure 1) can autonomously navigate at 60 *km/h* on-road and at 35 *km/h* off-road in daylight, and 15 *km/h* off-road at night or under inclement weather conditions. The vehicle employs the NIST developed 4D/RCS (**R**eal-Time **C**ontrol **S**ystem) [1] for autonomous navigation. The primary navigation suite of this vehicle consists of a Schwartz Electro-Optics **L**Aser **D**etection **A**nd **R**anging (LADAR), color cameras, **G**lobal **P**ositioning **S**ystem (GPS), and an **I**nertial **N**avigation **S**ystem (INS). The navigation system uses a Kalman filter to fuse data from the INS and the carrier phase differential GPS unit to compute the vehicle's position, orientation, speed, and velocity. GPS (even in differential mode) is not always reliable as the accuracy of the GPS estimates depends on the number of satellites in view. Hence to continually provide reliable vehicle information, an alternate solution becomes inevitable.

With increasing computing power and reduction in size

¹Certain commercial equipment, instruments, or materials are identified in this paper in order to adequately specify the experimental procedure. Such identification does not imply recommendation or endorsement by NIST, nor does it imply that the materials or equipment identified is necessarily best for the purpose.



Figure 1: The Demo III XUV is a hydrostatic diesel, 4 wheel drive, 4 wheel steer vehicle capable of autonomous navigation in unstructured and off-road driving conditions. The LADAR is shown in white.

and increase in sophistication of LADAR units, our motivation to register 3D LADAR data (both consecutive range images and also range images to *a priori* maps) is many fold:

- Firstly, LADAR registration can minimize the dependence on GPS and either serve as a primary navigation solution (in the absence or degradation of GPS) or as a secondary combined solution along with GPS.
- Within RCS, the use of *a priori* maps would enhance the scope of the world model. These maps may take a variety of forms including survey and aerial maps and may provide significant information about existing topology and structures. In order to take advantage of this knowledge, research is needed to register these *a priori* maps with the sensor-centric maps [4]. Additionally, for incorporating *a priori* knowledge into the world model, some form of weighting is required and this depends on how well the *a priori* data and the sensed information are registered.
- There is also the need to generate higher resolution *a priori* terrain maps as the current survey maps are too coarse for autonomous driving.

- Another potential application for registering LADAR data is the computation of *ground truth* as such registration is not dependent on time-based drift (unlike INS), vehicle maneuvers and terrain of travel.

All of the above mentioned factors warrant the need to develop robust 3D LADAR data registration algorithms. We have adapted the **I**terative **C**losest **P**oint (ICP) algorithm for registering the LADAR range images. At each iteration, the technique determines the closest match for each point and updates the estimated transformation based on a least-squares metric with some modifications to increase robustness. ICP and its variants have been widely used for registration purposes [9]. For autonomous vehicle navigation, ICP has been used for registration of range images for 3D terrain mapping [5] and localization [7]. Modified versions of the ICP algorithm have also been proposed for registration of range images in the presence of outliers [6],[8].

This paper is organized as below: Section 2 describes the registration of 3D LADAR data. Section 2.1 applies the ICP algorithm with suitable modifications to achieve sufficiently reliable registration of LADAR range images. Section 3 describes the experimental setup and provides the corresponding results. Section 4 concludes the paper outlining further research efforts.

2 Iterative Registration of 3D LADAR Data

We term the process of 3D LADAR data *registration* as:

Given two sets of 3D range image scan points (model set: \mathbf{M} and data set: \mathbf{D}): Find a 3D transformation (rotation and translation) which when applied to \mathbf{D} minimizes a distance measure between the two point sets.

The goal can be stated more formally as:

$$\min_{(\mathbf{R}, \mathbf{T})} \sum_i \|\mathbf{M}_i - (\mathbf{R}\mathbf{D}_i + \mathbf{T})\|^2 \quad (1)$$

where \mathbf{R} is a 3×3 rotation matrix, \mathbf{T} is a 3×1 translation vector and the subscript i refers to the corresponding points of the sets \mathbf{M} and \mathbf{D} .

We adapt the ICP algorithm for registering 3D LADAR range images. The algorithm as we have applied to register range images with suitable modifications is given in the next section.

2.1 Iterative Closest Point Algorithm

The ICP algorithm [3] can be summarized as follows: Given an initial motion transformation between the two 3D point sets, a set of correspondences are developed between data points in one set and the next. For each

point in the first data set, find the point in the second that is closest to it under the current transformation. It should be noted that correspondence between the two points sets is initially unknown and that point correspondences provided by sets of closest points is a reasonable approximation to the true point correspondence. From the set of correspondences, an incremental motion can be computed facilitating further alignment of the data points in one set to the other. This find correspondence/compute motion process is iterated until a predetermined threshold termination condition.

In its simplest form, the algorithm can be described by the following steps:

1. For each point in \mathbf{D} compute the closest point in \mathbf{M} from the set comprising $N_{\mathbf{D}}$ data and $N_{\mathbf{M}}$ model points. We tessellate \mathbf{M} using Delaunay triangulation and then do a 3D nearest point search. At the end of this step, we have all model points that correspond to data points and the distances between corresponding points.
2. Compute the incremental transformation (\mathbf{R}, \mathbf{T}) using Singular Value Decomposition (SVD) using correspondences obtained in step 1.
3. Apply the incremental transformation from step 2. to \mathbf{D} .
4. If relative changes in \mathbf{R} and \mathbf{T} are less than a threshold, terminate. Else go to step 1.

To deal with spurious points/false matches and to account for occlusions and outliers, we modify and weight the least-squares objective function in Equation (1) such that [11]:

$$\min_{(\mathbf{R}, \mathbf{T})} \sum_i p d_i \|\mathbf{M}_i - (\mathbf{R}\mathbf{D}_i + \mathbf{T})\|^2 \quad (2)$$

If the Euclidean distance between a point x_i in one set and its closest point y_i in the other, denoted by $d_i \triangleq d(x_i, y_i)$, is bigger than the maximum tolerable distance threshold \mathcal{D}_{max} , then $p d_i$ is set to zero in Equation (2). This means that an x_i cannot be paired with a y_i since the distance between reasonable pairs cannot be very big. The value of \mathcal{D}_{max} is set adaptively in a robust manner by analyzing distance statistics. Let $\{x_i, y_i, d_i\}$ be the set of original points, the set of closest points and their distances, respectively. The mean and standard deviation of the distances are computed as:

$$\mu = \frac{1}{N} \sum_{i=1}^N d_i; \quad \sigma = \sqrt{\frac{1}{N} \sum_{i=1}^N (d_i - \mu)^2}$$

where N is the total number of pairs. The pseudo-code for the adaptive thresholding of the distance \mathcal{D}_{max} is given below:

$$\text{if } \mu < \mathcal{D} \\ \mathcal{D}_{max}^{itn} = \mu + 3\sigma;$$

```

elseif  $\mu < 3\mathcal{D}$ 
 $\mathcal{D}^{itn}_{max} = \mu + 2\sigma$ ;
elseif  $\mu < 6\mathcal{D}$ 
 $\mathcal{D}^{itn}_{max} = \mu + \sigma$ ;
else  $\mathcal{D}^{itn}_{max} = \epsilon$ ;

```

where itn denotes the iteration number, \mathcal{D} is defined as the average distance between the scan points to be registered and is a function of the resolution of the LADAR data. In our implementation, \mathcal{D} was selected based on the following two observations: (i) If \mathcal{D} is too small, then several iterations are required for the algorithm to converge and several good matches will be discarded, and (ii) if \mathcal{D} is too big, then the algorithm may not converge at all since many spurious matches will be included. At the end of this step, two corresponding point sets, $\mathbf{P}_M:\{\mathbf{p}_i\}$ and $\mathbf{P}_D:\{\mathbf{q}_i\}$ are said to be established.

We recover the incremental 3D transformation (rotation and translation) of step 2. in the least-squares sense as follows [2]:

- Calculate $H = \sum_{i=1}^{N_D} (\mathbf{p}_i - \mathbf{p}_c)(\mathbf{q}_i - \mathbf{q}_c)^T$; ($\mathbf{p}_c, \mathbf{q}_c$) are the centroids of the point sets ($\mathbf{P}_M, \mathbf{P}_D$).
- Find the SVD of H such that $H = U\Omega V^T$.
- The rotation matrix relating the two point sets is then given by $\mathbf{R} = VU^T$.
- The translation between the two point sets is given by $\mathbf{T} = \mathbf{q}_c - \mathbf{R}\mathbf{p}_c$.

We iterate this process as stated in step 4. until the mean Euclidean distance between the corresponding point sets \mathbf{P}_M and \mathbf{P}_D is less than or equal to a predetermined distance or until a given number of maximum iterations is exceeded.

3 Experimental Setup and Results

LADAR data obtained from field trials conducted on an experimental site at the Fort IndianTown Gap, PA, is used to test the iterative algorithm. The XUV traversed vegetated and rugged terrain during the course of the field trials experiencing heavy pitching and rolling motion characteristic of travel over such undulating terrain. The LADAR was mounted on a pan/tilt platform to increase its narrow 20° field of view. The range of the tilt motion is $\pm 30^\circ$ resulting in an effective field of view of about 80° . The LADAR provides a range image of 32 rows \times 180 columns (16 facets) where each data point contains the distance to a target in the operating environment. Utilizing knowledge about the LADAR mount position and calibration factors, the range information provided by the LADAR is transformed to cartesian coordinates.

Figure 2(a) and (b) show a graphical representation of the model (\mathbf{M}) and data (\mathbf{D}) LADAR range images.

The XUV is also shown. For this data set, the point sets are obtained from consecutive LADAR scans. Figure 2(c) shows the registered range images and Figure 2(d) shows the closest point distance before and after registration.

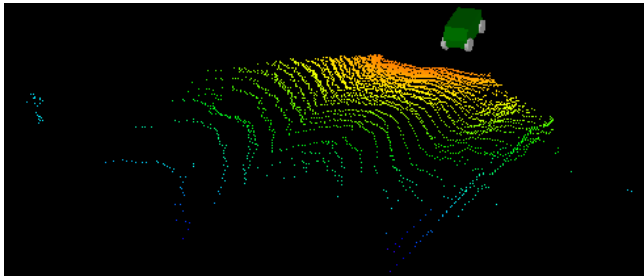
Figures 3(a) and (b) show the model and data range images before and after registration. To demonstrate the robustness of the proposed algorithm, range image \mathbf{D} was chosen to be 20 scans apart from the model range image and was also translated a meter along each of the (x, y, z) axes in addition to the translation and rotation that the image underwent due to the motion of the vehicle. It is important to note here that even though the range image points arrive in the same sequence for both the model and data sets, it is not guaranteed that both sets will have the same number of points as some facets of the LADAR data sets return empty values. As it can be seen from the Figures 3(a) and (b), the images are well registered after registration. Figure 3(c) shows a magnified view of the 3D nearest point search for correspondence determination midway through the registration process. The pairing of the model and data point sets can be clearly seen. Figure 3(d) depicts the closest point distance before and after registration of the range images. It is clear that after registration the distance between the range images have considerably reduced.

Table 1 summarizes the registration results for four data sets. Data sets #1 and #3 correspond to Figures 2 and 3, respectively. In data set #2, point sets separated by 20 scans were matched. In data set #4, range image \mathbf{D} of data set #1 was rotated 10 degrees and was also translated 3 meters along each of the (x, y, z) axes. Due to the above translation and rotation, it can be seen that both the number of iterations and the mean distance after registration have increased but the range images were still sufficiently registered. Note that such amounts of translation and rotation are highly unlikely to occur between consecutive range images as seen from Figure 2.

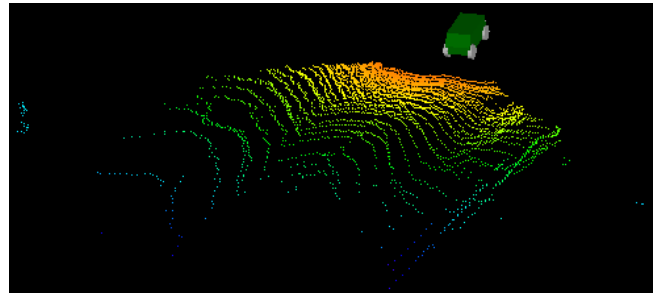
4 Conclusions and Further Work

The registration of 3D LADAR data for use in unmanned ground vehicle navigation was the main subject of this paper. An iterative algorithm for registering LADAR scans obtained from a moving XUV was described with suitable modifications to increase robustness. Field data obtained from experimental trials was used to test the efficacy of the algorithm in producing reliable results. The proposed iterative registration algorithm possesses the following strengths:

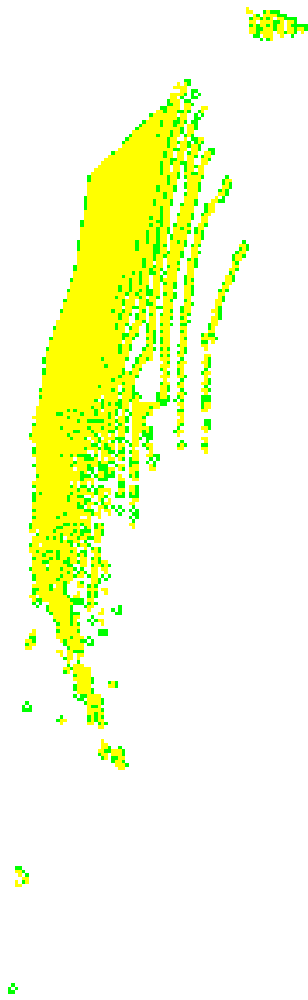
- It is iconic as it works directly on sensed data and thus does not require explicit extraction and matching



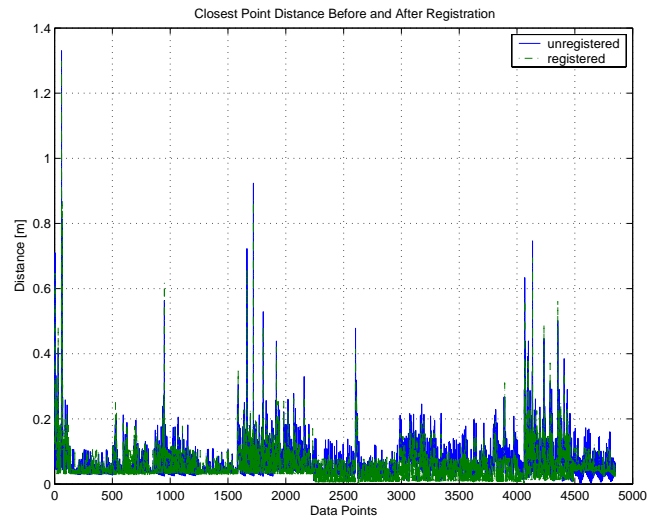
(a)



(b)



(c)



(d)

Figure 2: Model (M) and data (D) LADAR range images are shown in (a) and (b). The graphical front end depicted in (a) and (b) also shows the XUV as the range images were acquired. (c) shows the range images after registration. The closest point distance before and after registration of the range images is shown in (d).

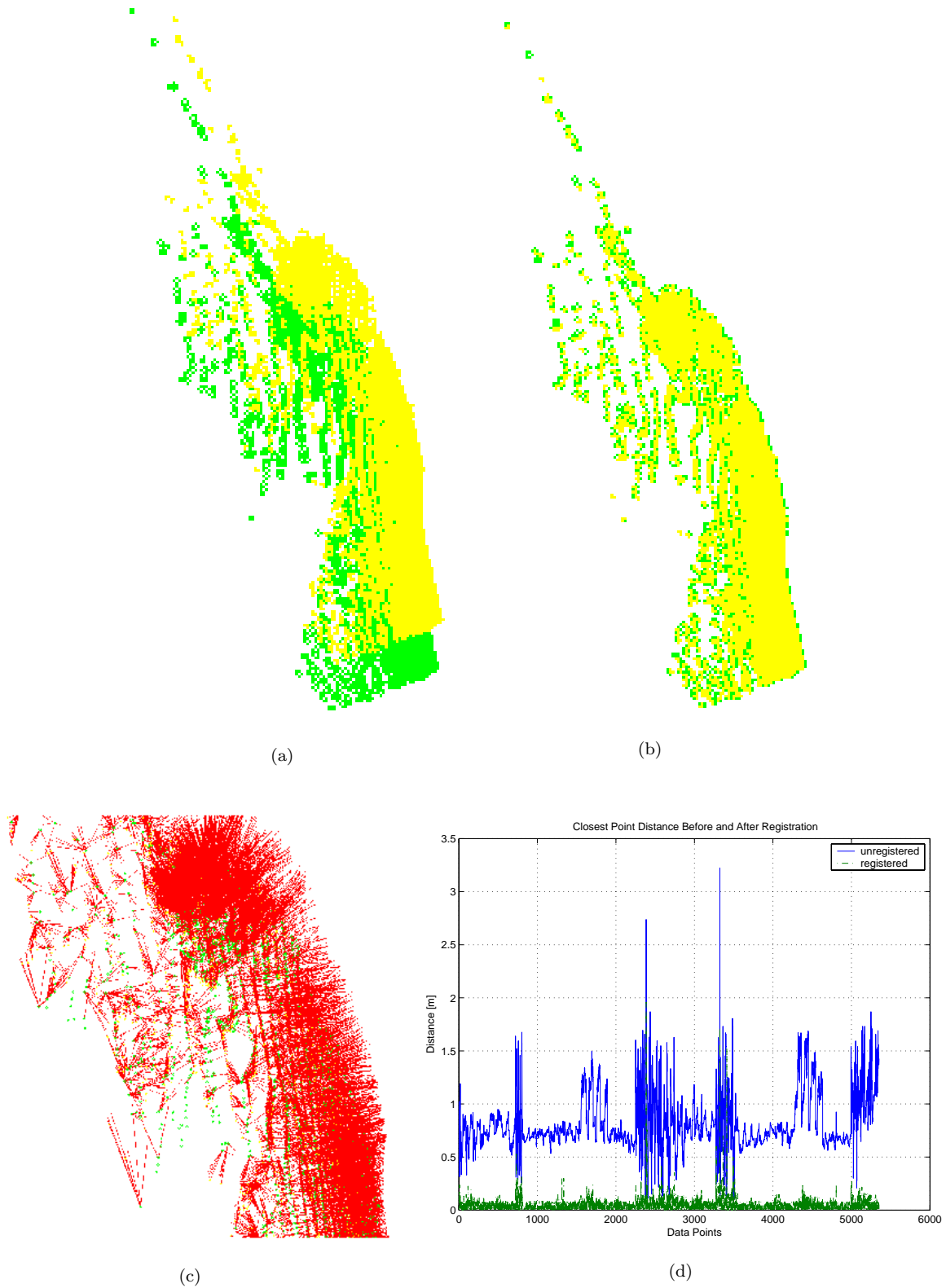


Figure 3: LADAR range images before (a) and after (b) registration. The data range image (**D**) was chosen to be 20 scans apart from the model range image (**M**) and was also deliberately translated 1 meter along the (x,y,z) axes in addition to the inherent translation to demonstrate the robustness of the iterative algorithm. (c) depicts a magnified view of the 3D nearest point search procedure for correspondence determination. (d) shows the closest point distance before and after registration of the range images.

Table 1: Quantitative Comparison of Performance

Data Set	Description	Mean Distance After Registration [cm]	# Iterations
#1 M:4852 D:4848	Consecutive scans	5.77	6
#2 M:5349 D:5352	20 scans apart	4.64	3
#3 M:5349 D:5352	$\mathbf{R}(0)\mathbf{T}(1)[\#2]$	4.64	38
#4 M:4852 D:4848	$\mathbf{R}(10)\mathbf{T}(3)[\#1]$	11.66	83

of features. Because the search is confined to small perturbations of the sensor scans, it is computationally efficient.

- The adaptive thresholding updating stage combined with least-squares technique yields reasonable registration even when there are false matches/spurious points and thus can deal with scenarios when the data is not a subset of the model, and
- It is robust to gross outliers and occlusions in the data.

Our future research efforts will concentrate on modifying the algorithm to extend it to real-time navigation and also in matching LADAR scans to *a priori* maps. Towards accomplishing these goals, the following areas are currently being investigated:

- **Global Minimization:** Even though ICP will only converge to the closest local minimum and there is no guarantee that this local minimum will correspond to the actual global minimum, convergence results are good for the tested field data. If wrong convergence proves to be an issue, stochastic optimization algorithms (e.g. Simulated Annealing) can be used to alleviate this problem. SA is extremely slow in converging to the global minimum and thus a hybrid algorithm that combines it with the proposed iterative algorithm would be more appropriate. As the convergence of the algorithm depends on an initial estimate, a sufficiently good initial estimate is required for superior registration. An initial estimate is almost always available in our case as it can be obtained from either the vehicle’s dead reckoning or GPS estimates.
- **Speed Enhancements:** Computing the correspondence is the most computationally expensive part of the algorithm. *kd-trees* have been proposed for faster correspondence where the complexity is reduced from $O(N_D N_M) \rightarrow O(N_D \log N_M)$ making the proposed algorithm real-time compatible. We have also employed Quaternions (instead of SVD) to determine the 3D transformation but it results only in a slight improvement in the resultant registration for the tested field trial data.
- **LADAR Uncertainty:** The quality of the 3D registration will significantly improve if the uncertainty of the LADAR range images are taken into account and has been so verified for 2D laser scan registration [7]. We are currently investigating the extension of these

results to the 3D case.

References

- [1] J. Albus et al. 4D/RCS Version 2.0: A Reference Model Architecture for Unmanned Vehicle Systems. Technical Report NISTIR 6910, National Institute of Standards and Technology, Gaithersburg, MD 20899, U.S.A., 2002.
- [2] K. Arun, T. Huang, and S. Bolstein. Least-Squares Fitting of Two 3-D Point Sets. *IEEE Transactions on Pattern Analysis and Machine Intelligence*, 9(5):698–700, 1987.
- [3] P. Besl and N. McKay. A Method for Registration of 3-D Shapes. *IEEE Transactions on Pattern Analysis and Machine Intelligence*, 14(2):239–256, 1992.
- [4] T. Hong, S. Balakirsky, E. Messina, T. Chang, and M. Shneier. A Hierarchical World Model for an Autonomous Scout Vehicle. In *Proceedings of the SPIE International Symposium on Aerospace/Defense Sensing, Simulation, and Controls*, pages 343–354, April 2002.
- [5] D. Huber, O. Carmichael, and M. Hebert. 3D Map Reconstruction from Range data. In *Proceedings of the IEEE International Conference on Robotics and Automation*, pages 891–897, 2000.
- [6] V. Koivunen, J. Vezien, and R. Bajcsy. Multiple Representation Approach to Geometric Model Construction from Range Data. Technical Report MS-CIS-93-66, GRASP Lab., University of Pennsylvania, 1993.
- [7] R. Madhavan. *Terrain Aided Localisation of Autonomous Vehicles in Unstructured Environments*. PhD thesis, The University of Sydney, January 2001. Available from <http://www.dissertation.com/library/1121776a.htm>, ISBN: 1-58112-177-6.
- [8] T. Masuda and N. Yokoya. A Robust Method for Registration and Segmentation of Multiple Range Images. In *Proceedings of the Second IEEE CAD-based Vision Workshop*, pages 106–113, 1994.
- [9] S. Rusinkiewicz and M. Levoy. Efficient Variants of the ICP Algorithm. In *Proceedings of the International Conference on 3-D Digital Imaging and Modeling*, pages 145–152, 2001.
- [10] C. Shoemaker and J. Bornstein. The Demo III UGV Program: A Testbed for Autonomous Navigation Research. In *Proceedings of the IEEE ISIC/CIRA/ISAS Joint Conference*, pages 644–651, September 1998.
- [11] Z. Zhang. Iterative Point Matching for Registration of Free-Form Curves and Surfaces. *International Journal of Computer Vision*, 13(2):119–152, 1994.